Comparative Evaluation of Seismic Assessment Methodologies Applied to a 32-Story Reinforced Concrete Office Building

Ali M. Memari[1], Shahriar Rafiee[2], Alireza Y. Motlagh[3] and Andrew Scanlon[4]

1. Department of Architectural Engineering, The Pennsylvania State University, 104 Engineering A Building, University Park, PA 16802, USA, email: amm7@psu.edu
2. P.O. Box 14665-175, Tehran, Iran
3. Department of Civil and Environmental Engineering, New Jersey Institute of Technology, University Heights, Newark, NJ 07102, USA
4. Department of Civil and Environmental Engineering, The Pennsylvania State University, 212 Sackett Building, University Park, PA 16802, USA

ABSTRACT: *Results of seismic damage evaluation of a tall reinforced concrete building are presented. Plastic hinge formation patterns obtained by using DRAIN-2D and IDARC computer programs for dynamic analysis are compared. Damage indices given by IDARC are interpreted and their implications compared with those of drift ratios. Results of static push-over analysis are compared with those of inelastic dynamic time history analysis. Moreover, the result of collapse mechanism approach is compared with that of static push-over analysis. It is shown that simple collapse mechanism approach can predict the failure mode given by static push-over analysis for this building. It is concluded that drift limits in codes do not necessarily predict the degree of damage that this type of construction can sustain in severe earthquakes.*

Keywords: Damage analysis; Nonlinear analysis; Push-over analysis

1. Introduction

Due to increasing awareness of the vulnerability of constructed facilities in the event of damaging earthquakes, seismic assessment of existing structures, in particular buildings designed according to older codes, has become increasingly important in structural engineering practice. An essential element in many seismic evaluations is the determination of ultimate inelastic response of the structure. Computer programs such as *DRAIN-2D* [7] that perform inelastic dynamic time history analysis (*IDTHA*) have the capability to trace the inelastic response during a prescribed input motion and report ductility parameters such as maximum plastic rotations in structural members. Traditionally, ductility factor has been used for evaluation of the extent of inelastic response or damage [17]. With respect to ductility, seismic safety of an existing building or a new design would be evaluated by comparing the demand ductility with some predetermined allowable value.

With further development of methodologies that incorporate more sophisticated damage models [11, 19], and release of computer programs that provide damage indices for seismic evaluation, e.g., *IDARC* [20], it is ex pected that the use of such tools will be more frequent than the use of programs that report only ductility demand based on inelastic dynamic time-history analysis.

There is a growing interest in application of nonlinear static analysis, known today as the push-over analysis [12, 16]. This method is currently being used in some cases as a substitute approach for *IDTHA*, despite its inability to evaluate dynamic response effects. As an alternative to sophisticated computer-based analysis, simple plastic analysis approaches based on a static collapse mechanism have been proposed [18] that give an estimate of ultimate inelastic response which can be used as the basis for design or evaluation. The present paper provides a review of available assessment criteria and illustrates the application of several approaches to seismic evaluation of a tall reinforced concrete frame-tube structure.

2. Objectives and Scope

The objectives of the study described in this paper were to demonstrate the application of several seismic assessment methodologies to a 32-story office building and to compare the results obtained by these methodologies. The scope of the study included analysis of the structure by static collapse mechanism as well as static, and dynamic analyses using available software packages and

application of assessment criteria reported in the literature to the results.

3. Assessment Criteria

A number of different parameters have been proposed to assess the seismic performance of building structures. These include drift ratio, which is a measure of lateral displacement of the structure, ductility factor, which is a measure of maximum inelastic response, and damage index, which considers both maximum inelastic response and dissipation of energy during the input motion.

3.1. Drift Ratio

The average drift, taken as the roof displacement divided by the building height is sometimes used to evaluate seismic performance. A value of 2% is usually considered as the threshold of extensive damage in most buildings. As an example of such a limit, *NEHRP* [2] specifies the allowable inelastic drift ratio to be 2% for a typical framed office building. It should be mentioned, however, that some documents have a different point of view and 2% is not a universally agreed upon value.

3.2. Ductility Factor

Ductility factor defined as the ratio of maximum deformation to initial yield deformation can be evaluated at the structure level (displacement ductility), member level (rotational ductility) and the section level (curvature ductility). Ductility factor can be used as an assessment criterion in the static collapse mechanism analysis, pushover analysis, and *IDTHA*. A check on ductility can also be made by computing the plastic rotation demand in members and comparing the demand with calculated available rotation capacity. The plastic hinge rotation capacity, θ_p, can be determined as

(1)

where and ϕ_y are the ultimate and yield curvatures at the critical section calculated using moment curvature analysis with the consideration of axial force as applicable, and is the length of plastic hinge. In this study, the material models used in the moment curvature analysis were those of Kent and Park [8] for confined concrete and Burns and Siess [3] for reinforcing steel. The plastic hinge length (L_p) used in Eq. (1), as suggested by Priestley and Park [23], is given by $(0.08z + 6d_b)$, where z is the distance from critical section to the point of contra-flexure assumed to be $\frac{1}{2}$ of the clear member length and d_b is the diameter of the longitudinal reinforcement. It should be mentioned that steel strength can also be considered in this relation for more accurate calculation of L_p.

3.3. Damage Index

For a rational seismic assessment of an existing building, the analysis model should incorporate most aspects of nonlinear behavior that can have a bearing on the response. While, earlier *IDTHA* programs, e.g. *DRAIN-2D* [7], base damage assessment on comparison of ductility demand and the corresponding deformation capacity, more advanced damage models consider the potential of the structure to plastically dissipate the inherent hysteretic energy in addition to the ductility. As a representative of these models, the Park and Ang damage model [19], which, according to Williams et al [28], is one of the most accurate ones, is used in this study. In this model, structural damage in an element is expressed as a function of the ductility and the hysteretic energy in the form of a damage index D_i as follows:

$$D_i = \delta_m / \delta_u + (\beta / \delta_u P_y) \int dE \qquad (2)$$

where δ_m is the maximum deformation response, δ_u is the ultimate deformation capacity under monotonic loading, P_y is the yield strength, dE is the incremental absorbed (dissipated) hysteretic energy (excluding the stored potential energy), and β, which measures the strength degradation rate, is defined as the ratio of incremental damage resulting from the increase in maximum response to normalized incremental hysteretic energy. While and $\int dE$ are obtained from *IDTHA*, δ_u, P_y, and depend on the result of a static analysis, with parameters and β obtained from empirical expressions based on test results [29].

The local damage index, corresponds to an element. The damage index for a story and the structure as a whole is obtained by summing component contributions, that is, $D = \sum \lambda_i D_i$, where λ_i is the weighting factor defined as the ratio of total energy absorbed (including the stored potential energy) by element *i* to total energy absorbed in the story or the structure.

According to the *IDARC* manual [20], damage index less than 0.4 indicates extensive but repairable cracking in concrete. A damage index between 0.4 and 1.0 indicates likelihood of damage beyond repair (e.g., crushing of concrete and buckling of reinforcement). The building can be considered partially or totally collapsed for a damage index greater than 1.0.

4. Analysis Methods

To evaluate the response of a structure to earthquake motion, several available analytical techniques can be applied. In the present study, analyses were performed using the static collapse mechanism approach, linear elastic time history analysis, static pushover analysis, and inelastic time history analysis as described below.

4.1. Static Collapse Mechanism Analysis

In the static collapse mechanism approach [18], it is assumed that the design displacement ductility factor, μ_Δ, defined as the ratio of maximum inelastic response, Δ_u, to the displacement at first yield, Δ_y, can be approximated as the ratio of maximum (roof) elastic displacement, Δ_e, to the displacement caused by the application of code prescribed seismic loads, Δ_{code}. This assumption is based on the equal displacement hypothesis [17]. In order to proportion and detail structural members such that the specified displacement ductility can be achieved, rotation or curvature demands in members should be established. In the case of seismic assessment of existing buildings, it is necessary to compare the plastic hinge rotations associated with top lateral displacement with the available plastic hinge rotation capacities. It can be assumed that when the structure enters the yielding state, plastic hinges form at the ends of members. The larger the specified displacement ductility, the larger will be the amount of plastic hinge rotations. In order to estimate the corresponding plastic hinge rotations, we can conveniently assume that all plastic hinges form at the same load and enough plastic hinges form to develop a single degree of freedom collapse mechanism. A relation between the design displacement ductility and plastic hinge rotations can be developed based on kinematics. After assuming a suitable sidesway mechanism, we can develop expressions for Δ_y and Δ_u as functions of beam and/or column curvatures and lengths. By dividing the expression for Δ_u by that for Δ_y, the desired relationship between design displacement ductility and column and/or beam curvatures or plastic hinge rotations is determined.

4.2. Static Nonlinear Push-Over Analysis

The objective of static push-over analysis [4, 12, 24, 26] is to determine nonlinear response (forces and deformations) of the structure up to a point that is determined a priori to correspond to a certain degree of damage or to the response level associated with the design earthquake. The static nonlinear step-by-step analysis is performed by subjecting the structure incrementally to a loading system with a predetermined pattern, usually representing the first mode response in the shape of an inverted triangle. Regardless of the lateral load pattern type, the loading level is increased until the maximum top (roof) displacement reaches a certain percentage of building height or some other prescribed stopping criterion. By using appropriate force deformation models for critical sections, the extent and distribution of inelastic deformation at the local element level is determined.

4.3. Linear Elastic Dynamic Time History Analysis

The program *ETABS* [5] provides a 3*D* analysis of a multi-story structure under the assumption that the floor acts as a rigid diaphragm. The *ETABS* analysis results are discussed in detail by Memari et al [14]. The results for story displacement will be used in comparison with inelastic analysis results to evaluate the equal-displacement hypothesis.

4.4. Inelastic Dynamic Time History Analysis

Two computer programs, *DRAIN*-2*D* and *IDARC*, were selected to perform inelastic dynamic analysis. The element library of *DRAIN*-2*D* includes a reinforced concrete beam element with strength deterioration in addition to strain hardening. The computer program *IDARC* is capable of carrying out nonlinear static collapse analysis, inelastic dynamic time-history analysis, and a comprehensive damage analysis for *R/C* buildings as described in Section 3.3. The hysteretic model used in *IDARC* is capable of modeling strength deterioration and pinching effect in addition to stiffness degradation.

5. Evaluation of a 32-Story Office Building

The assessment criteria and analysis methods described above were applied to an existing reinforced concrete structure. Results obtained are outlined in the following sections.

5.1. Building Description

The structure for this study is a 32-story reinforced concrete building in downtown Tehran. It has a height of 101.51*m* above grade and plan dimensions of 34.5*m* in the *N-S* and 36.0*m* in the *E-W* directions. Figure (1) shows a photograph of the building and Figure (2) shows a typical plan view of the structure. The lowest three stories are below grade and serve as parking levels. The floor system consists of a 6*cm* reinforced concrete slab supported by reinforced concrete 11*cm* wide by 40*cm* deep joists at 50*cm* on centers. The slab has increased thickness of 20*cm* between column lines 3 and 4 along the corridor adjacent to elevator shafts and stair cases. The floor system for the top two stories has an added 7*cm* thick lower slab under the joists, forming a sandwich type system. The joists are supported by two *E-W* direction shallow beams (40*cm* deep, 110*cm* wide) along column lines 2 and 5, 20*cm* thick walls along column lines 3 and 4, and the exterior framing system.

Perimeter columns are spaced at 1.5*m* and are framed by spandrel beams with a depth of 1.1*m*. In the end portions of *N-S* direction frames, there are shear walls each spanning five column lines. The foundation consists of a 1.7*m* thick solid mat, and 70*cm* thick *R/C* perimeter basement walls. The interior frames and walls are gravity bearing systems, leaving essentially the perimeter frames to resist lateral loads by a combination of tube action [9]

and frame action. The tube action, which resists the overturning tendency, is manifested by the compressive and tensile forces generated mostly in the columns of perpendicular frames. The frame action, which resists shear due to lateral forces, is brought about by the flexure in beams and columns of the parallel frames.

5.2. Seismic Forces and Input Motions

The inelastic dynamic time-history analysis (*IDTHA*) was performed using three earthquake ground motion records [15]. The records are accelerograms of Tabas *N* 16 *W* Sept. 16, 1978 ($PGA = 0.93g$), Naghan Longitudinal April 16, 1977 ($PGA = 0.72g$), and El Centro *N-S* May 18, 1940 ($PGA = 0.32g$). The first two records are implicity specified by the Iranian Standard 2800 [1], as maximum credible earthquakes regardless of the site location in Iran. The third one is used here for comparison purposes.

Analyses were performed for both the unscaled records and for scaled records for which all three records were scaled to peak ground acceleration values of $0.3g$ to $0.5g$ at $0.05g$ intervals for comparison purposes. Although some researchers (e.g., [27]) do not favor normalization of the records to the same *PGA*, others (e.g., Lawson et al [12]) find scaling the records to some peak acceleration beneficial for comparison purposes. Other methods of

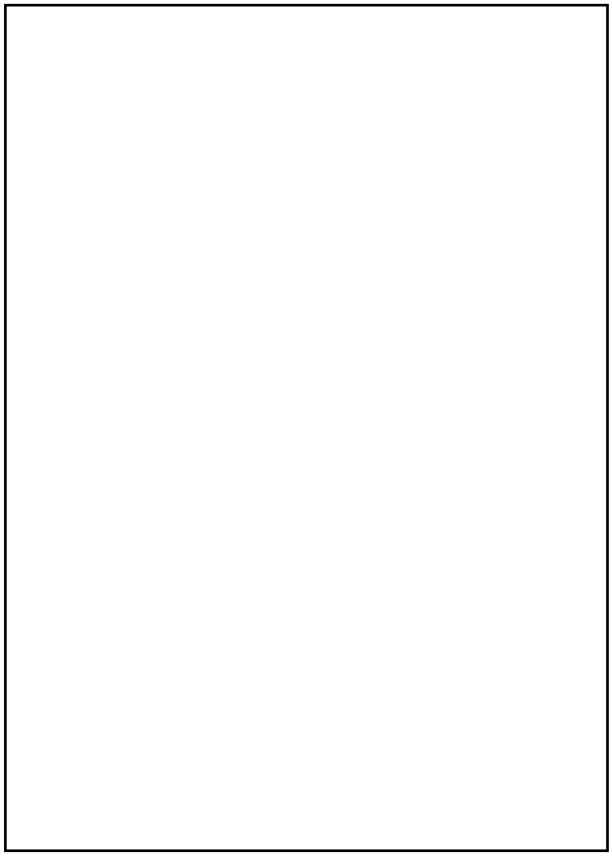

Figure 1. A photograph of the building.

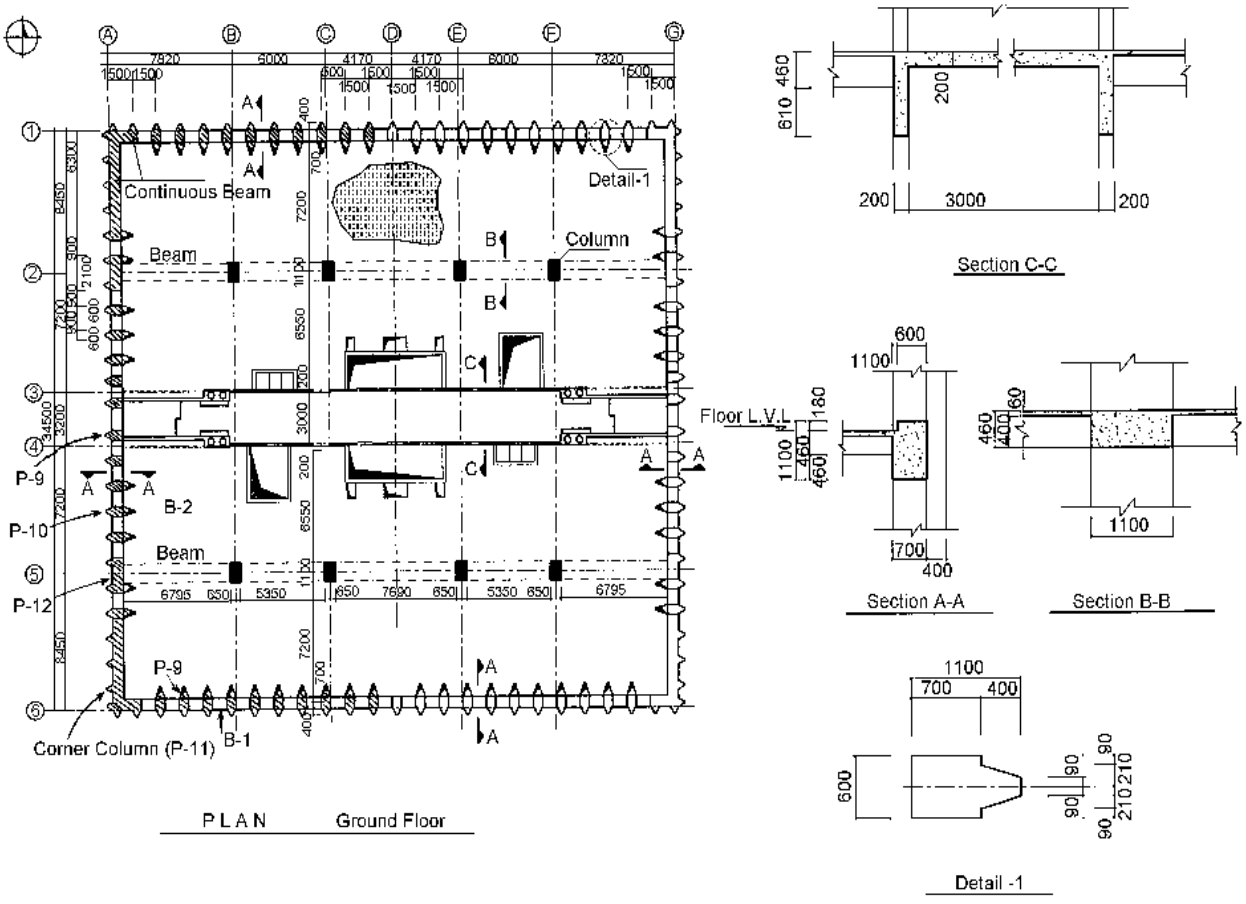

Figure 2. Building plan and some details.

scaling to obtain equal values of spectrum intensity have also been suggested [6, 13]. In addition to analysis of these input motions the building was analyzed [14] for the equivalent static lateral force method prescribed in seismic code Standard 2800 [1].

5.3. Static Collapse Mechanism Analysis

Static collapse mechanism analysis is suggested by Priestley [21] to serve as a method that gives results that are consistently reliable as compared with the previous more sophisticated methods. As mentioned in Section 3, to perform a static collapse mechanism analysis, it is necessary to establish a relation between top lateral displacement ductility factor and plastic hinge rotation or curvature ductilities corresponding to a probable collapse mechanism. The two basic simple collapse mechanisms are a column sidesway mechanism when column critical sections develop yield before beams and a beam sidesway mechanism when beams commence yield before columns. More specifically, as shown in Figure (3), a column sides-way mechanism is defined such that plastic hinges form at top and bottom of all columns of a story. A beam sidesway mechanism is defined when plastic hinges form at critical sections of all beams in the frame and the bottom of first story columns. For most buildings, a mixed sidesway mechanism, shown also in Figure (3), will probably be the actual failure mechanism [22].

$\mu_{\phi c}$

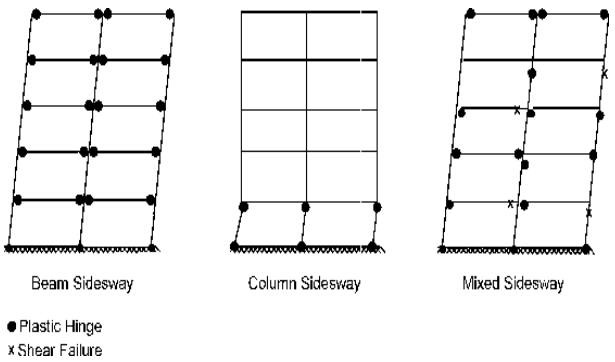

Figure 3. Definition of collapse mechanisms.

In this work, since the approximate collapse mechanism was determined by the static push-over analysis, only the column sidesway and beam sidesway mechanisms were pursued to determine how close the prediction is to the more accurate mechanism predicted by push-over analysis. Moreover, based only on these two mechanisms, it is of interest to make an assessment of the building and compare result with that of push-over analysis. Based on the expression suggested by Park and Paulay [18], the following relationships were developed to express beam and column curvature ductility demands in terms of a specified displacement ductility factor

$$\mu_{\phi c} = 2.9(\mu_{\Delta} - 1) + 1 \quad (3)$$

$$\mu_{\phi b} = 6.4(\mu_{\Delta} - 1) + 1 \quad (4)$$

As explained in Section 3, the displacement ductility factor can be approximated as the ratio of displacement resulting from linear elastic time history analysis to that resulting from the seismic code prescribed equivalent static lateral force method. For this analysis, the result of *ETABS* based 3-*D* linear elastic analysis [14] is used. The top displacements resulting from *N-S* direction time history analysis using the three records as input in addition to the displacement resulting from the seismic code Standard 2800 [1] prescribed equivalent static lateral force method are listed in Table (1). The top displacement ductility factors, also listed in Table (1), are obtained by dividing the dynamic analysis results by the equivalent static result. The curvature ductility capacity for perimeter beams obtained using curvature capacities (mentioned subsequently) varies between 22 and 40, with a mean value of 31. As can be seen in Table (1), the beam curvature ductility demand is in the range of 11.8 to 45.8, or approximately from 1/3 to $1\frac{1}{2}$ times the average capacity. Considering the approximations involved in the process, this means that when compared to the column situation as is discussed next, the beams are not critical based on this analysis. To determine ductility capacity for columns, we need to assume a compressive axial force level corresponding to which ductility capacity is determined. For example, for column type *P*-9, subject to the code level force of 494 *ton* corresponding to the ground story, we get curvature ductility capacity of 2.7. Similarly, for column type *P*-10, at axial force level of 590 *ton*, the result is 2.1. The range of curvature ductility demand at the ground story is 5.9 to 21.3 or roughly from 2.2 to 7.9 times the capacity for column type *P*-9 and 2.8 to 10.1 times the capacity for column type *P*-10. Obviously, this indicates that even if we disregard the possibility of a more potentially damaging column sideways mechanism, the columns are still critical in the assumed beam sidesway mechanism.

Table 1. Displacement and curvature ductilities.

Seismic Input	Δ_{max} (cm)	μ_{Δ}	$\mu_{\phi b}$	
Equivalent Static	7.9	1.0	-	-
El Centro Record	21.1	2.7	11.8	5.9
Naghan Record	33.5	4.2	21.8	10.4
Tabas Record	62.8	8.0	45.8	21.3

The prediction here is that the columns do not have sufficient rotation capacities and if we were to push the building gradually to failure, columns of the ground story would form plastic hinges before beams and thus the failure mechanism would be closer to a column sidesway mechanism. As mentioned before, this mode is consistent with the relative strength of beams and columns in the lowest story. The same result was obtained by the static push-over analysis.

5.4. Static Nonlinear Pushover Analysis

Modeling of the building for *IDARC* analysis is discussed in detail by Rafiee [25]. For brevity, only key assumptions are mentioned here. Since the plan is approximately symmetrical, only one half of the building is modeled for *N-S* direction analysis. The primary lateral load resisting system for the half of the structure is the *N-S* perimeter frame that along with he two *E-W* half-frames at the north and south ends effectively will behave as a vertical channel and provide resistance to overturning mechanism, with one half-frame in tension and the other in compression. The gravity load resisting system consists of interior columns, stair-case, elevator shaft walls, and the perimeter frame. The interior walls have not been designed for lateral load resistance and, therefore, are not considered to be effective in the inelastic lateral load-resisting model. During the elastic response range, these walls contribute to the stiffnesses of the building. However, during inelastic response, their stiffness can be assumed to be significantly reduced because of cracking. Figure (4) shows a schematic description of various elements used in *IDARC*. The diaphragm in each floor is assumed to be rigid in its own plane and is modeled by using rigid elements (running *N-S*), each connecting one column of the south side half frame to the corresponding column (on *N-S* column lines) on the north side half frame (Figure (2)). Beams and columns are modeled using prismatic beam and column elements. Special edge column [30] are employed at the corner columns in order to account for large axial forces their due to tube action [10]. These elements are modeled in the program as one-dimensional axial springs. Moreover, special transverse beam elements, which offer torsional stiffness in addition to resistance to vertical deformation, are employed to model beams connecting the two *E-W* half-frame columns. This, in effect, engages the perpendicular two *E-W* half frames with the main *N-S* frame.

In the analysis under consideration, at each stage of loading interval, an inelastic analysis has been performed and displacements calculated. The collapse load in this analysis is taken to correspond to the state where top deformation exceeds 2% of the building height. It should be noted that with 2% average drift, some stories will have

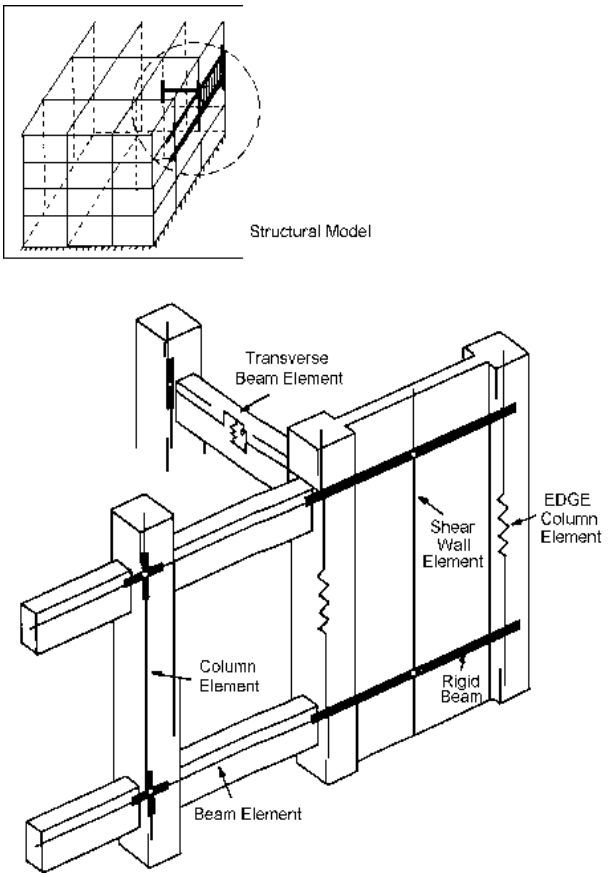

Figure 4. Schematic description of finite elements available in *IDARC* as shown in the *IDARC* manual [29].

higher story drifts. The result of static push-over analysis is presented in Figure (5) in the form of variation of base shear coefficient (base shear divided by the building weight) with deformation at the top in terms of percent of the height of the building. This plot is the result of the application of a monotonic loading with triangular distribution to the building. Figure (5) shows only a portion of load-deformation curve, where it can be seen that the curve is leveling off at a top building displacement of about 1.25% of the height. According to this diagram, the lateral load is still growing at a displacement of 1.25% of the height, but the growth rate is very slow.

The static push-over analysis also provides the mode of failure at ultimate strength. Figure (6) shows the distribution of plastic hinges and cracked sections in the frame under consideration. The failure pattern indicates that most of the columns in the lower sixth of the frame have yielded. The figure also shows that much fewer beams than columns have formed plastic hinges. The obvious conclusion is that throughout this structure, columns form plastic hings before beams and the failure mechanism is expected to be close to column sway type. The lowest story seems to almost form a soft story sway failure. An evaluation of the moment capacity of beams and columns, reported in Memari et al [14], revealed that beams in the first story are three times as strong as

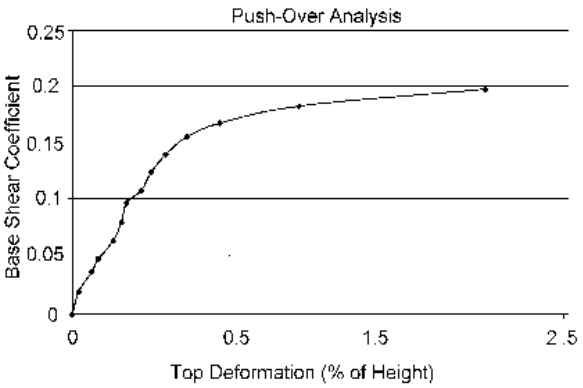

Figure 5. Result of push-over analysis by IDARC.

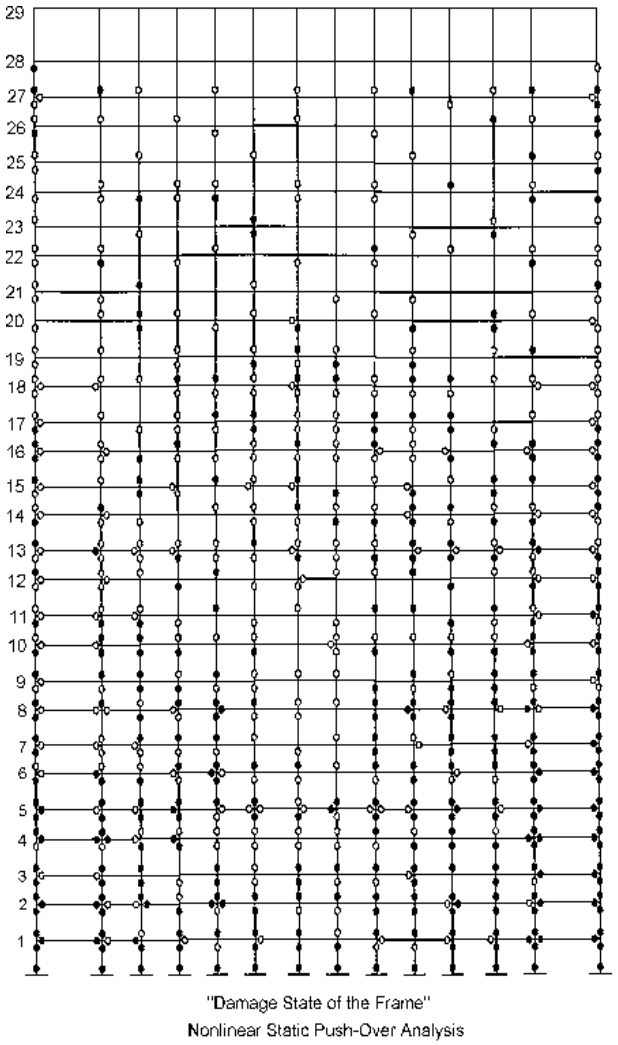

Figure 6. Distribution of plastic hinge formations and cracked sections resulting from IDARC push-over analysis.

columns. The pattern of plastic hinge formation shown in Figure (6) is consistent with the information and indicates that columns have yielded before beams.

5.5. Inelastic Dynamic Time History Analysis

Details of the modeling of the subject building based on *IDTHA* using *DRAIN*-2*D* are discussed by Memari et al [15]. Some of the results of *DRAIN*-2*D* analysis are used here to compare with the results based on *IDARC* analysis. In summary, due to plan symmetry, one half of the building is modeled for analysis. Beam-column elements with concentrated plasticity at the ends and strain hardening characteristics are used for column and wall members. As a comparison for column plastic hinge formation, we consider the criteria in *DRAIN*-2*D* first. Accordingly, a plastic hinge forms in a beam-column when the demand (*M, P*) falls on or outside the boundary of the failure surface. *DRAIN*-2*D* analyses were performed using all three input records. To demonstrate the types of results obtained, plastic rotations for column *P*-9 are plotted in Figure (7). Plotted also in this figure are the ultimate rotation capacities determined using Eq. (1) and based on moment-curvature relations for the critical section with consideration of the axial load effect and concrete confinement. Dead load, live load, and earthquake loads have been combined without load factors in the *DRAIN*-2*D* analysis to determine the axial load effects used in calculation of rotation capacities. Plastic hinge formation in *DRAIN*-2*D* occurs in beam elements when $M > M_y$ and in column elements when the point (*P, M*) falls on or outside of the failure surface. Plastic hinge formation in *IDARC* occurs when $M > M_y$. *IDARC* does not consider *P-M* interaction while *DRAIN*-2*D* considers that in an approximate sense for beam-column element. The results of the *DRAIN*-2*D* analyses are discussed further in Section 6.

In the initial analysis by *IDARC*, all three records were scaled to peak ground acceleration values of 0.3*g* to 0.5*g* at 0.05*g* intervals for comparison purposes. Based on the results of such analyses, *IDARC* determined overall damage indices for the structure as a whole. The result is shown in Table (2). It can be seen that the damage indices for the El Centro record are larger than the respective values for Tabas and Naghan records when the *PGA* is the same for all three records. The reason for this can be related to the existence of wider spikes (longer duration pulses) in the El Centro record that can cause greater damage than narrower spikes in the other two records. By plotting the damage indices versus *PGA*, it is possible to obtain estimates for overall damage index as a function of *PGA* for this building, as shown in Figure (8). Using this figure, we can get an estimate for the bounds of damage index associated with probable earthquakes with *PGAs* between 0.3*g* and 0.5*g*. The figure shows that there is roughly a linear relation between damage index and peak ground acceleration, with a slope in the range of 11.0 to 12.0 for the three cases shown.

The overall structure damage index is determined as a weighted sum of the story indices and each story index is in turn determined as a weighted sum of the component indices. The result of member damage indices for a portion

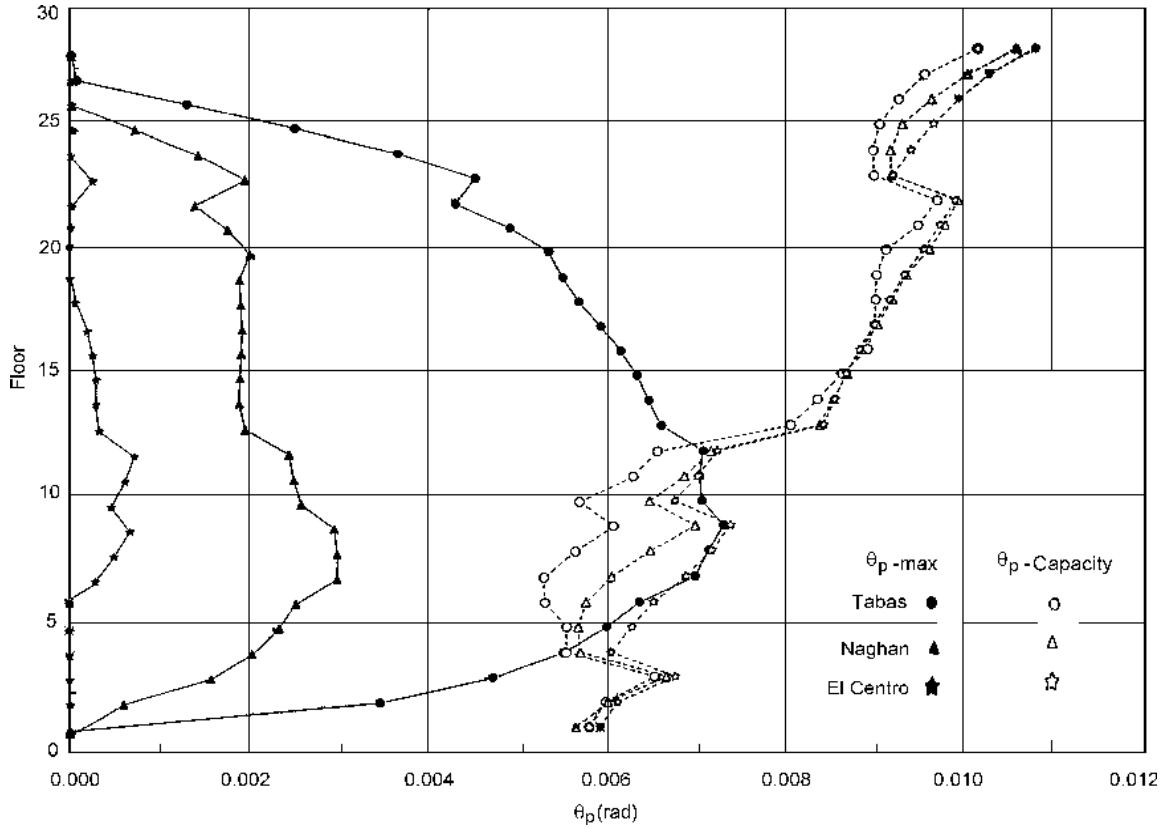

Figure 7. Distribution of plastic hinge rotation demand resulting from DRAIN-2D and plastic hinge rotation capacity for column P-9.

Table 2. IDARC damage indices for the building as a whole with normalized records.

PGA	Naghan	Tabas	El Centro
0.30g	0.15	0.21	0.24
0.35g	0.23	0.26	0.32
0.40g	0.28	0.31	0.37
0.45g	0.33	0.35	0.44
0.50g	0.39	0.43	0.49

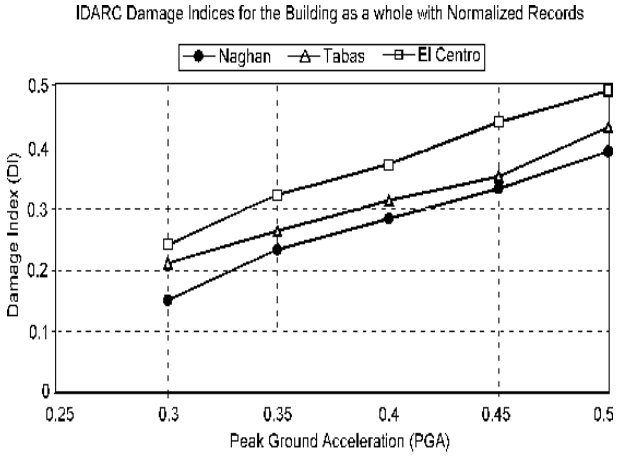

Figure 8. Relation between damage indices and peak ground acceleration.

of the structure for El Centro record with *PGA* of 0.3*g* is shown in Figure (9). Different values were obtained for Tabas and Naghan records with the same *PGA*. With such differences in component damage indices, it can be concluded that such indices are rather sensitive to the frequency content and the duration of the excitation. The latter, however, will be important if is such that the energy dissipated is crucial.

It may be of interest to see how the relation between strength of the structure and demand based on spectral accelerations compare with these results. Based on three dimensional linear elastic analysis of the same building [14] subjected to linear elastic response spectra for *PGA* = 0.3*g*, 0.4*g* and 0.5*g*, the demand-capacity ratio for base shear turned out to be 2.08, 2.72, and 3.51, respectively. This information, which if plotted shows a near linear relation, gives the slope of the demand-capacity ratio versus *PGA* of approximately 7.2. This value is about 40% smaller than the slope in Figure (8). It should be noted that although the latter results from linear elastic analysis, the slope is on the same order as that for the former. The comparison reveals that there is an approximate linear relation (in the range shown) between the response (damage index or base shear) and *PGA*.

Separate analyses were also made using the unscaled records. The overall damage indices are 0.27, 0.68, and 0.94 for El Centro, Naghan, and Tabas records, respectively. According to these indices and considering

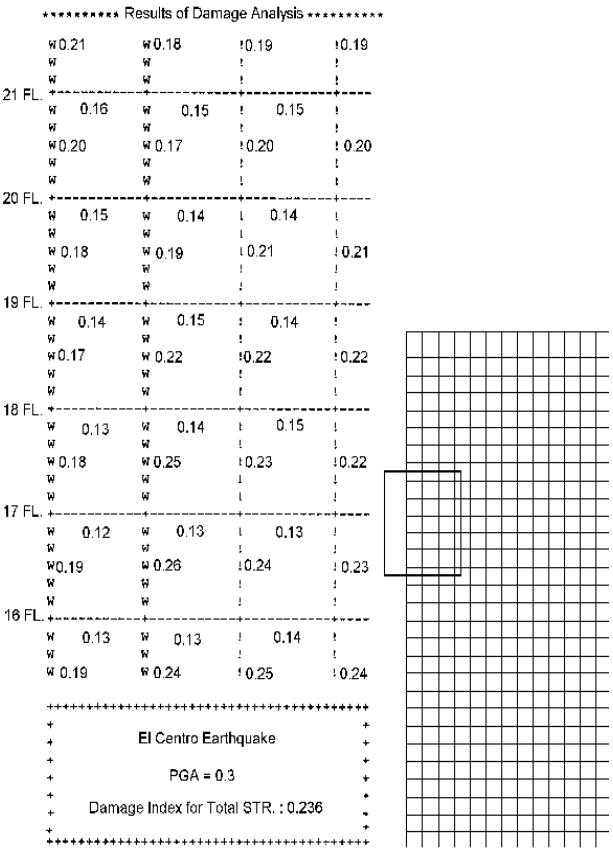

Figure 9. Member damage indices for a portion of the building frame.

the interpretation of damage index values mentioned before, the building would be at the threshold of collapse, would sustain damage beyond repair, and would have repairable damage if it were to experience, respectively, Tabas, Naghan, and El Centro earthquakes of the resulting failure modes showing the pattern of plastic hinge formation the one corresponding to the Tabas record is shown in Figure (10) as an example. As expected, the extent of plastic hinge formation is more critical for the case of Tabas record than the other two. The first story shows a near column sway mechanism due to Tabas record, as almost all columns in that story indicate plastic hinge formation, but only some of the beams have yielded at the ends. In general, there are more plastic hinges in the joints on the two most exterior columns, which are the locations of column types *P*-11 and *P*-12 (Figure (2)). The failure pattern due to El Centro record had much fewer plastic hinge formations. In general, the overall damage indices mentioned previously show consistency with the extent of plastic hinge formations in Figure (10).

In order to compare the conclusions drawn from damage indices with the more conventional rule of thumb based on relative story displacement or drift ratio, we can look at the resulting distribution of maximum story displacements due to the three records, as shown in Figure (11). The average drift ratio (top displacement

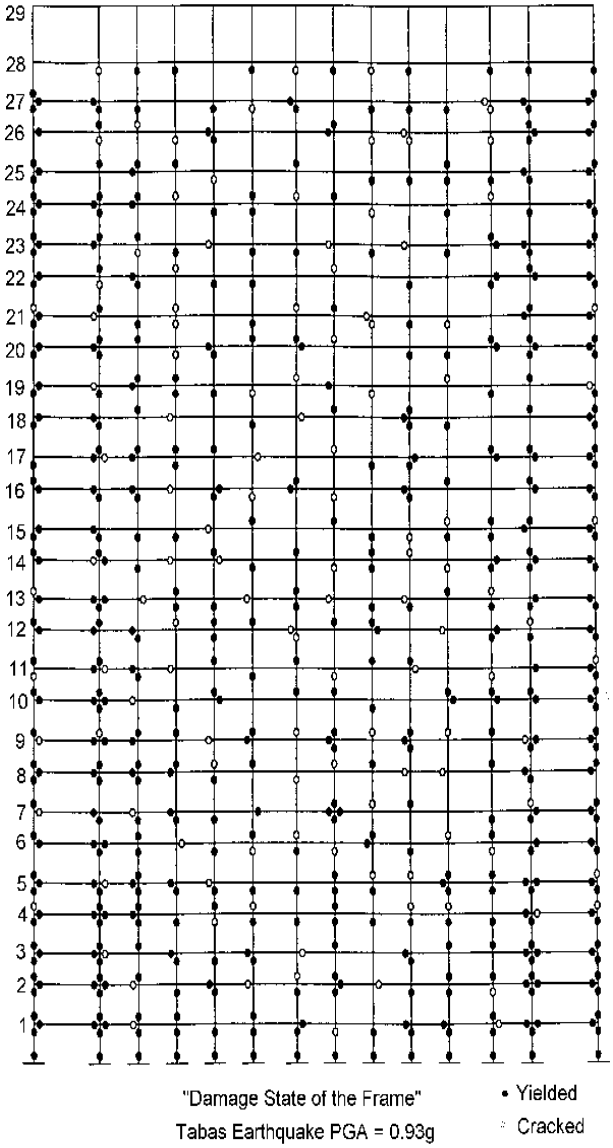

Figure 10. IDARC result--distribution of plastic hinge formations and cracked sections.

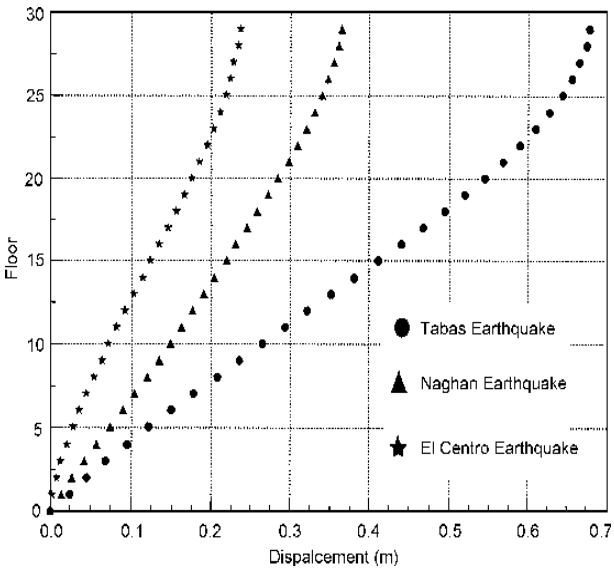

Figure 11. IDARC result-story displacements due to the three records.

divided by building height) due to El Centro, Naghan, and Tabas is , respectively, 0.2%, 0.4% and 0.7%. The drift ratio for Tabas is much smaller than 2% which is usually considered as the threshold of extensive damage in most buildings. Considering the possibility of extensive plastic hinge formation due to Tabas record, one can expect that the structure will sustain considerable structural damage were it subjected to this earthquake. Such a possibility, however, is not readily obvious from the drift ratio value of 0.7% which would mean the possibility of nonstructural damage in a conventional framed building. Yagi et al [29] point out to somewhat similar result. They show that for a 41-story reinforced concrete tube building considerable number of plastic hinges formed in beams when the story drift ratio was 0.5%. Plastic hinges did not form in columns since weak beam-strong column criterion was implemented in design. Given that the damage indicates can provide a more accurate measure of damage than the 2% rule of thumb, it is possible to correlate the drift rations due to the three earthquake records with the overall structure damage indices, so as to have a better interpretation of the drift ratio values for this type of building. This is shown in Figure (12). Such a relation shows the possibility of serious structural damage to this kind of building construction at drift ratios much less than the code allowable value.

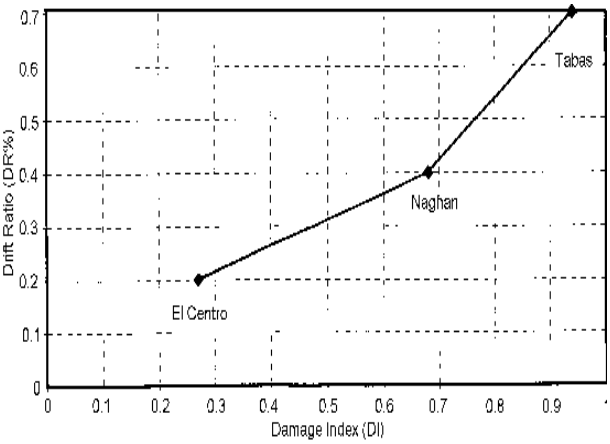

Figure 12. Relation between average drift ratio and damage index for the three records.

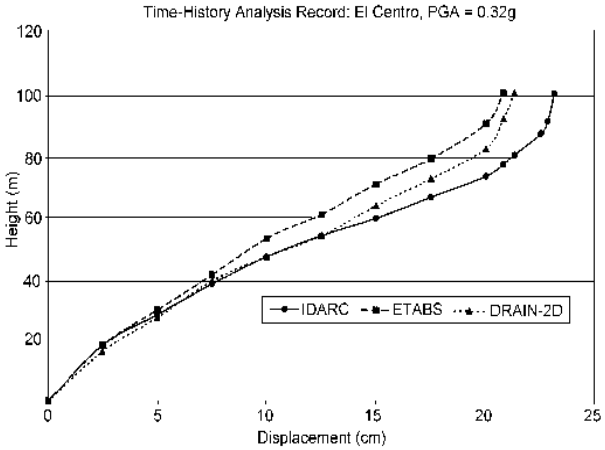

Figure 13. Comparison of story displacement distribution resulting from IDARC, DRAIN-2D, and ETABS time-history analysis using El Centro record.

6. Comparison of Results by Different Methods

Results obtained by the selected analysis techniques are compared in this section. Of particular interest are comparisons of story displacements and plastic hinge development.

6.1. Story Displacements by Dynamic Analysis

Story displacement diagrams resulting from *DRAIN*-2*D* and *IDARC* under the action of El Centro record are plotted in Figure (13). Using this figure, not only story displacements, but also average inter-story drifts can be compared. The distributions of displacements are the same up to the mid-height of the building. Beyond that, IDARC displacements are slightly larger, with the maximum difference of 10% at the top. The difference is partially due to the difference in section force-deformation modeling in *IDARC* and *DRAIN*-2*D*.

It is also of interest to compare these inelastic analysis results with the one based on linear elastic dynamic time history analysis using *ETABS* [5], as shown in the same figure. The analysis results are discussed in detail by Memari et al [14]. It can be seen that the *ETABS* displacement distribution is closer to a linear response, with *ETABS* displacements being generally smaller than those of *DRAIN*-2*D*. The displacement at the top obtained by *ETABS* is smaller than those of *DRAIN*-2*D* and *IDARC*, respectively, by 2.8% and 13.8%, but with the maximum respective differences of 13.5% and 14.3% at the 19th story (at height of 65*m*). The average inter-story drift (top displacement divided by building height) is 0.203% for *ETABS*, 0.209% for *DRAIN*-2*D*, and 0.227% for *IDARC*. Such ratios show that the average inter-story drift resulting from *ETABS* is smaller than those of *DRAIN*-2*D* and *IDARC*, respectively, by 2.9% and 10.6%. Although these percentages (2.9% and 10.6%) are relatively close to those obtained by top displacement (2.8% and 13.8%), inter-story drifts are usually used as the main global performance parameters. It is interesting to note that the equal displacement hypothesis [17] considered to be applicable for buildings with periods greater than 0.5sec, is almost verified when we compare the maximum displacement obtained by *ETABS* and *DRAIN*-2*D* but it is somewhat cruder when we compare *ETABS* with *IDARC*. This can partly be attributed to the difference in modeling used in the two programs (*DRAIN*-2*D* and *IDARC*). It should also be noted that these results are due to El Centro record.

It can be expected that if the comparison is made for stronger earthquake records that cause more extensive nonlinear response, the results discussed might be different.

6.2. Plastic Hinge Formation

Figure (14) shows the plastic hinge formation in selected columns determined by *DRAIN*-2*D* and *IDARC* due to the Tabas Earthquake record as an example for the three records. The information provided on the figure is limited to the column lines shown for brevity and clarity of the figure. Moreover, the information about the location (top and/or bottom) of plastic hinges is not shown on this figure since only the column count (not the plastic hinge count) with at least one plastic hinge is of interest in this discussion.

The agreement, with regard to the location where plastic hinges form, is good for Tabas, fair for Naghan, and poor for El Centro records (results not shown for the latter two). Apparently, the larger the *PGA*, the better the agreement between the two programs for this particular case. However, it should be noted that the plot indicates the columns that have yielded. In other words, for portions that there seems to be inconsistency, the actual values of the rotations or moments could be close to, but not quite exceeding, the yield value.

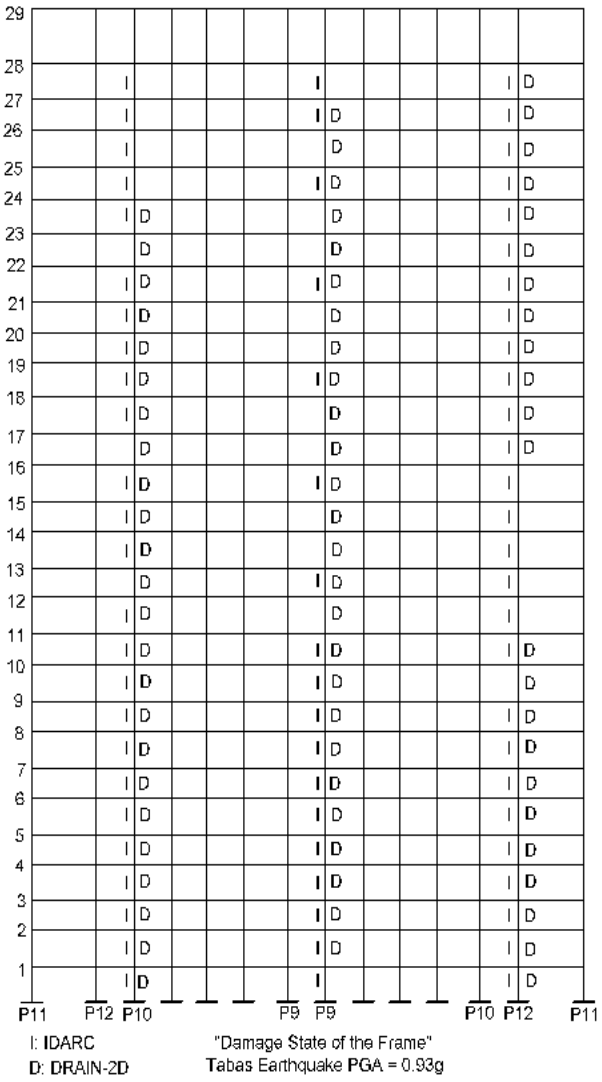

Figure 14. Comparison of plastic hinge formation resulting from IDARC and DRAIN-2D in selected columns.

It should also be noted that formation of a plastic hinge does not necessarily constitute complete failure in the column unless transverse reinforcement is poor. As can be seen in Figure (7), the available column rotation capacities to tolerate the incurred plastic rotations is considerable. At points where $\theta_p > \theta_u$, however, complete failure of the column can be expected.

Since static push-over analysis is now commonly used as an alternative to nonlinear dynamic analysis, it is of interest to compare the results obtained by both approaches. Although the top displacement is not the same in the push-over analysis and dynamic analysis results, the two analysis results can be compared on the basis of formation of plastic hinges as an indication of the potential failure mode. Based on the number of plastic hinge formations, static push-over analysis has caused fewer yield sections than those caused by the Tabas record. Thus dynamic excitation has caused more beams to yield than the static push-over analysis.

Although the plastic hinge formations in dynamic analysis is not simultaneous, as it is usually assumed in the static analysis, nonetheless, the pattern of the plastic hinges formed by the two methods can reveal some useful information. To compare the pattern of plastic hinge formation due to the application of the three records and static push-over analysis, Figure (15) shows distribution of plastic hinge formation in the columns of the frame with at least one plastic hinge (top and /or bottom). The plastic hinge formation pattern resulting from the static push-over case is in better agreement with those of the dynamic analysis results (associated with Tabas and Naghan records) in the lower half of the frame in terms of the location and number of columns forming plastic hinges. The difference is larger in the upper half stories. One basic explanation for the difference is that the combined effects of the dynamic characteristics of the structure and the attributes of each records (e.g., peak acceleration, frequency content, and length of record) create unique plastic hinge formation patterns in each dynamic analysis case, where in general it cannot be predicted by the static collapse analysis. However, as far as the total number of columns with plastic hinges is concerned, a simple observation is that the static push-over analysis predicted approximately 23% less than those due to Tabas ($PGA = 0.93g$), 7% more than those due to Naghan ($PGA = 0.72g$), and 88% more than those due to El Centro ($PGA = 0.32g$). If the total number of columns with at least one plastic hinge can be considered to have a direct relation to damage potential, then one can draw preliminary

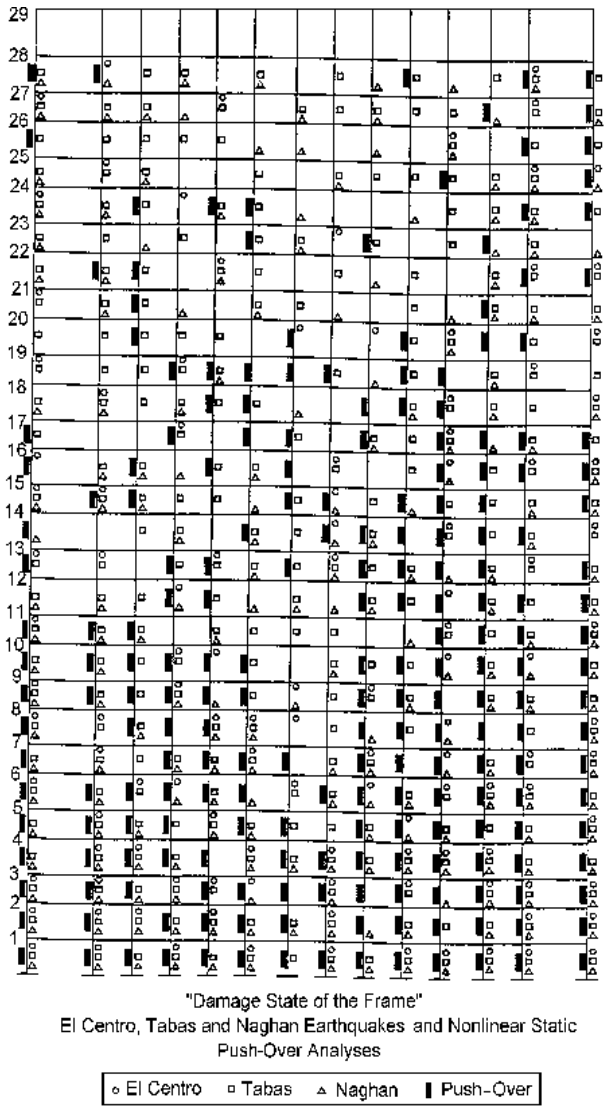

Figure 15. Comparison of distribution of plastic hinge formation resulting from IDARC time-history analyses with push-over analysis.

conclusions regarding the damage potential of earthquakes with different *PGAs*. In other words, the result in this example indicates how well a static push-over analysis may predict the response obtained by a nonlinear dynamic analysis, and it is obvious that the prediction can vary widely depending on the *PGA* of the input.

Another observation here is that the maximum top displacement due to static push-over analysis, which was set to 2% of the building height (2.03*m*), is approximately three times that due to Tabas records (0.675*m*). Yet, as mentioned above, column plastic hinge formations due to static push-over analysis is 23% smaller. This can be explained by noting that in the push-over analysis, static lateral loads are applied gradually forcing the building to deflect more in the first mode shape, while the maximum deflection in the dynamic analysis includes the effect of higher modes which has a definite impact on taller buildings.

7. Summary and Conclusions

Based on the results of the study reported in this paper, some general conclusions can be drawn with respect to the methods involved and criteria used. With respect to assessment criteria it appears that the 2% rule of thumb for maximum inelastic drift is overly optimistic for framed tube buildings of this type and a value of about 1% or less might be more appropriate. The overall damage index obtained from *IDARC* analyses seems to provide a good qualitative indication of the onset of collapse during a severe earthquake. The ductility demand capacity comparison also provides useful information about potential performance during a severe earthquake. Following are some specific conclusions of this paper:

- The average inter-story drift ratio for Tabas record with *PGA* of 0.93*g* and damage index of 0.94 is 0.7% which is much smaller than the conventionally accepted 2% as the threshold of extensive damage for most buildings.
- The results show that it is possible that damage indices indicate the potential for severe damage to a building, while the resulting small values of inter-story drift do not reveal that possibility. Conversely, relatively small values of average inter-story drifts for certain types of buildings could correspond to potentially severe structural damage.
- The *IDARC* results show that there is approximately a linear relation between damage index and *PGA*.
- The pattern of plastic hinge formation are somewhat different according to *DRAIN*-2*D* and *IDARC* for the models of this particular building, with better agreement for larger *PGA*.
- *IDARC* analysis resulted in 10.6% larger displacement at the top compared to *DRAIN*-2*D* result for El Centro record.
- The maximum top displacement results form *DRAIN*-2*D* and *IDARC* are respectively, 2.8% and 13.8% larger than a three-dimensional linear elastic analysis using *ETABS*. The average inter-story drift resulting from *ETABS* are smaller than those of *DRAIN*-2*D* and *IDARC*, respectively, by 2.9% and 10.6% for this building.
- The prediction of plastic hinge formation by push-over analysis appears to be in general agreement with the dynamic analysis results especially in the lower half stories, with better agreement for larger *PGA*.
- With respect to the total number of columns with at least one plastic hinge, the static push-over analysis predicted 23% fewer than those due to Tabas, 7% more than those due to Naghan, and 88% more than those due to El Centro record.
- The static collapse mechanism analysis predicted

roughly the same type of failure mode as that by push-over analysis.

Acknowledgments

This study was supported by International Institute of Earthquake Engineering and Seismology (IIEES) and Bank Saderat in Tehran. The work was primarily performed at Sharif University of Technology and IIEES.

References

1. Building and Housing Research Center (BHRC) (1988). "Iranian Code for Seismic Resistant Design of Buildings", Standard 2800, Publication No. 82, 5th Ed., Tehran.

2. Building Seismic Safety Council (BSSC) (1994). "NEHRP Recommended Provisions for the Development of Seismic Regulations for New Buildings", Washington, D.C.

3. Burns, N.H. and Siess, C.P. (1962). "Load-Deformation Characteristics of Beam-Column Connections in Reinforced Concrete", Civil Engineering Studies, Structural Research Series No. 234, University of Illinois.

4. Fajfar, P. and Gaspersic, P. (1996). "The N2 Method for the Seismic Damage Analysis of RC Buildings", *Earthquake Engineering and Structural Dynamics*, **25**, 31-46.

5. Habibullah, A. (1986). "Extended Three Dimensional Analysis of Building Systems", *Computers and Structures, Inc.*, Berkeley, CA.

6. Housner, G. (1952). "Spectrum Intensities of Strong-Motion Earthquakes", *Proceedings of the Symposium on Earthquake and Blast Effects on Structures*, Los-Angeles, CA, 20-36.

7. Kanaan, A.E. and Powell, G.H. (1973). "DRAIN-2D-A General Purpose Computer Program for Dynamic Analysis of Inelastic Plane Structures with Users' Guide", Earthquake Engineering Research Center, Report UCB/EERC-73/22, Berkeley, CA.

8. Kent, D.C. and Park, R. (1990). "Flexural Members with Confined Concrete", *Journal of Structural Division*, *ASCE*, **97**, ST 7, 1969-1990.

9. Khan, F.R. and Amin, N.R. (1973). "Analysis and Design of Framed Tube Structures for Tall Concrete Buildings", *Response of Multistory Concrete Structures to Lateral Forces*, ACI/SP 36-3, 39-60

10. Kim, S.D., Hong, W.K., and Ju, Y.K. (1999). "A Modified Dynamic Inelastic Analysis of Tall Buildings Considering Changes of Dynamic Characteristics", *The Structural Design of Tall Buildings*, **8**, 57-73.

11. Krawinkler, H. and Zohrei, M. (1982). "Cumulative Damage in Steel Structures Subjected to Earthquake Ground Motions", *Computers and Structures Journal*, **16**(1-4), 531-541.

12. Lawson, R.S., Vance, V., and Krawinkler, H., (1994). "Nonlinear Static Push-over Analysis-Why, When, and How?", *Proceedings of Fifth U.S. National Conference on Earthquake Engineering*, Chicago, 283-292.

13. Martinez-Rueda, J.E. (1998). "Scaling Procedure for Natural Accelerograms Based on a System of Spectrum Intensity Scales", *Earthquake Spectra*, **14**(1), 135-152.

14. Memari, A.M., Motlagh, A.Y., Akhtari, M., Scanlon, A., and Ghafory-Ashtiany, M. (1999). "Seismic Vulnerability Evaluation of a 32-Story Reinforced Concrete Building", *Structural Engineering and Mechanics Journal*, **7**(1), 1-18.

15. Memari, A.M., Motlagh, A.Y., and Scanlon, A. (2000). "Seismic Evaluation of an Existing Reinforced Concrete Framed Tube Building Based on Inelastic Dynamic Analysis", *Engineering Structures Journal*, **22**(6), 621-637.

16. Naeim, F. and Lobo, R. (1999). "Avoiding Common Pitfalls in Push-Over Analysis", *Proceedings of 8th Canadian Conference on Earthquake Engineering*, Vancouver, 269-274.

17. Newmark, N.M. and Hall, W.J. (1973). "Proceedings and Criteria for Earthquake Resistant Design", *Building Practice for Disaster Mitigation*, Building Science Series 46, National Bureau of Standards, Washington, D.C., 209-236.

18. Park, R. and Paulay, T. (1975). "*Reinforced Concrete Structures*", John Wiley & Sons.

19. Park, Y.-J., Ang, A.H.-S., and Wen, Y.K. (1985). "Seismic Damage Analysis of Reinforced Concrete Buildings", *Journal of Structural Engineering*, *ASCE*, **111**(4), 740-757.

20. Park, Y.-J., Reinhorn, A.M., and Kunnath, S.K. (1987). "IDARC: Inelastic Damage Analysis of Reinforced Concrete Frame--Shear-Wall Structures", National Center for Earthquake Engineering Research, Technical Report NCEER-87-0008, SUNY at Buffalo.

21. Priestley, M.J.N. (1997). "Displacement-Based Seismic Assessment of Reinforced Concrete Buildings",

Journal of Earthquake Engineering, **1**(1), 157-192.

22. Priestley, M.J.N. and Calvi, G.M. (1991). "Towards a Capacity Design Assessment Procedure for Reinforced Concrete Frames", *Earthquake Spectra*, Earthquake Engineering Research Institute, **7**(3), 413-437.

23. Priestley, M.J.N. and Park, R. (1987). "Strength and Ductility of Concrete Bridge Columns Under Seismic Loading", *ACI Structural Journal*, **84**, 61-76.

24. Qi, X. and Moehle, J.P. (1991). "Displacement Design Approach for Reinforced Concrete Structures Subjected to Earthquakes", UCB/EERC-91/02, Earthquake Engineering Research Center, Berkeley, CA.

25. Rafiee, S. (1995). "Comparative Study of Different Methods that Consider Nonlinear Dynamic Behavior of Tall Reinforced Concrete Buildings Subject to Strong Earthquakes", Master of Science Thesis (in Farsi), Sharif University of Technology, Tehran.

26. Saiidi, M. and Sozen, M.A. (1981). "Simple Nonlinear Seismic Analysis of R/C Structures", *Journal of Structural Division, ASCE*, **107**(ST 5), 937-951.

27. Shome, N. and Cornell, C.A. (1998). "Normalization and Scaling Accelerograms for Nonlinear Structural Analysis", *Proceedings of 6th US NCEE*, Washington, CD-Rom.

28. Williams, M.S., Villemure, I., and Sexmith, R.G. (1997). "Evaluation of Seismic Damage Indices for Concrete Elements Loaded in Combined Shear and Flexure", *ACI Structural Journal*, **94**(3), 315-322.

29. Yagi, S., Yoshioka, K., Eto, H., and Nishimura, K. (1990). "Seismic Design of a 41-Story Reinforced Concrete Tube Structure", *Proceedings of 4th World Congress, Tall Buildings: 2000 and Beyond,* Council on Tall Buildings and Urban Habitat, Hong Kong, 1123-1137.